



## ANALYSIS OF AN ALL SPEED METHOD IN LAMINAR FLOWS USING UNSTRUCTURED MESHES

**Wladimir M. C. Dourado**

Centro Técnico Aeroespacial, Instituto de Aeronáutica e Espaço  
CTA/IAE/ASA-P, 12228-904 – São José dos Campos – SP – BRASIL

**João Luiz F. Azevedo**

Centro Técnico Aeroespacial, Instituto de Aeronáutica e Espaço  
CTA/IAE/ASE-N, 12228-904 – São José dos Campos – SP – BRASIL

**Abstract.** *An improved numerical scheme to calculate all speed flows on unstructured meshes is presented. The Navier-Stokes equations are solved both for internal and external laminar flows. Three channel configurations are used to validate the scheme to internal flows and a flat plate with different Reynolds numbers is used to validate for external flows. The results are compared with analytical solutions and numerical solutions presented at the literature.*

**Key Words:** *Fluid mechanics, Numerical methods, Aerodynamics, All speed methods.*

### 1. INTRODUCTION

A large number of reasons can be enumerated in order to show the advantage of unified computational fluid dynamics methods which are able to treat very low speed flows, as well as high speed flows. The authors have discussed these ideas in the past (Dourado and Azevedo, 1996), emphasizing the advantages of all speed methods to treat low speed flows. The implementation of the all speed method in the unstructured grid context was derived from still earlier work using structured grids (Azevedo and Martins, 1993; Martins and Azevedo, 1993; Martins, 1994; Ferrari and Azevedo, 1995; Ferrari, 1995). In the present work, the objective is to perform a validation of the capability to simulate laminar viscous flows with the proposed methodology.

The paper briefly presents the formulation adopted, using the Navier-Stokes equations written in the conservative form. There is no addition of turbulence models, since the flowfields of interest are assumed to be laminar. The numerical method is also presented with emphasis in the implementation of the artificial dissipation terms. The work has demonstrated that a careful definition of these terms, especially in the wall proximity, is fundamental in order to achieve good quality results. Moreover, special attention was dedicated to boundary condition implementation. In the authors' experience and as also discussed by Mavriplis (1990), this is crucial to the correct reproduction of the flow phenomena.

The numerical method was validated using both internal and external flow test cases. The flow over a flat plate was considered as the external flow test case. Results are compared in this case with Blasius' analytical solution for the problem. Flow in a 2-D channel is the internal flow

test case. In this case, the development of the velocity profile along the channel provides a form of comparison with other numerical data in the literature (Chen and Pletcher, 1991). Problems that arose, during the present effort, due to less than optimum discretization of boundary layer regions are also discussed in the paper.

## 2. FLOW EQUATIONS AND SPATIAL DISCRETIZATION

The adequate formulation to describe the phenomena are the Navier-Stokes equations in integral and conservative form. For two dimensional flow, they are written as

$$\int_V \frac{\partial Q}{\partial t} dV + \oint_S (E_e \vec{i} + F_e \vec{j}) \cdot \vec{n} dS = \oint_S (E_v \vec{i} + F_v \vec{j}) dS , \quad (1)$$

where  $Q$ ,  $E_e$ ,  $F_e$  are the conservative flow properties and Euler convective flow vectors in the Cartesian directions  $x$  and  $y$ , respectively as well as  $E_v$  and  $F_v$  are the viscous flow vectors in these directions, respectively. These vectors are presented in Dourado and Azevedo (1996). The viscous terms that appear in the expressions of  $E_v$  and  $F_v$  can be written as

$$\begin{aligned} \delta_{xx} &= -p - \frac{2}{3}\mu \vec{\nabla} \cdot \vec{V} + 2\mu \frac{\partial V_x}{\partial x} , \\ \delta_{yy} &= -p - \frac{2}{3}\mu \vec{\nabla} \cdot \vec{V} + 2\mu \frac{\partial V_y}{\partial y} , \\ \tau_{xy} &= \mu \left( \frac{\partial V_y}{\partial x} + \frac{\partial V_x}{\partial y} \right) , \end{aligned} \quad (2)$$

where  $\vec{V}$  is the velocity vector with Cartesian components  $V_x$  and  $V_y$ , and  $\mu$  the molecular viscosity coefficient.

To couple pressure and velocity in those equations, the gasdynamic relation for total energy  $e$  is used and can be written in the following way:

$$e = \frac{p}{\gamma - 1} + \frac{1}{2}\rho (V_x^2 + V_y^2) , \quad (3)$$

where  $e$  is the total energy per unit of volume,  $p$  is the static pressure and  $\rho$  is the density. For very low speed flow, density variations are very small and, therefore, it would be interesting to have the continuity equation written in terms of another variable. If one could accomplish this change of dependent variables, then it would be possible to use standard compressible flow schemes, such as those described in Jameson, Schmidt and Turkel (1981) and Jameson and Mavriplis (1986), to solve Eq. (1). The set of dependent variables adopted in this work is

$$q = \{p, u, v, T\} . \quad (4)$$

In the present work, the vector  $q$  will be referred to as the vector of primitive variables. With introduction of a Jacobian to make the variable substitution, Eqs. (1) can be rewritten adopting the set of primitive variables and the resulting equations are

$$\int_V \mathcal{D} \frac{\partial q}{\partial t} dV + \oint_S (E_e \vec{i} + F_e \vec{j}) \cdot \vec{n} dS = \oint_S (E_v \vec{i} + F_v \vec{j}) dS , \quad (5)$$

where  $\mathcal{D} = \partial Q / \partial q$  is the Jacobian matrix relating conserved and primitive variables. Both Eulerian and viscous flux vectors in this equations are now written as a function of the primitive variables in Eq. (4). Further details of the method can be found in Azevedo and Martins (1993), Martins and Azevedo (1993) and Dourado and Azevedo (1996)). Moreover, details of the unstructured cell vertex discretization of the governing equations can also be found in Dourado and Azevedo (1996). The adimensionalization of equations follows the work presented by Chen and Pletcher (1991).

### 3. NUMERICAL METHOD: TIME MARCHING

The time integration of Eqs. (5), to reach steady state, is based in an explicit, modified Runge-Kutta time-marching scheme, following the philosophy presented in earlier works of Jameson and Mavriplis (1986) and Mavriplis (1988). Explicit methods permit easier parallelization as well as they are a cheaper driver to multigrid methods. Although the present work does not use multigrid acceleration, the code is already being prepared for this type of enhancement in the future. The five-stage hybrid time-stepping scheme used for time integration is given by

$$\begin{aligned}
 q^{(0)} &= q^n \\
 q^{(1)} &= q^{(0)} - \alpha_1 \frac{\Delta t}{\Omega} \mathcal{D}^{-1} \left[ C \left( q^{(0)} \right) - D_0 \right] \\
 q^{(2)} &= q^{(0)} - \alpha_2 \frac{\Delta t}{\Omega} \mathcal{D}^{-1} \left[ C \left( q^{(1)} \right) - D_1 \right] \\
 q^{(3)} &= q^{(0)} - \alpha_3 \frac{\Delta t}{\Omega} \mathcal{D}^{-1} \left[ C \left( q^{(2)} \right) - D_2 \right] \\
 q^{(4)} &= q^{(0)} - \alpha_4 \frac{\Delta t}{\Omega} \mathcal{D}^{-1} \left[ C \left( q^{(3)} \right) - D_3 \right] \\
 q^{(5)} &= q^{(0)} - \alpha_5 \frac{\Delta t}{\Omega} \mathcal{D}^{-1} \left[ C \left( q^{(4)} \right) - D_4 \right] \\
 q^{n+1} &= q^{(5)} .
 \end{aligned} \tag{6}$$

The  $D_i$  operators which appear in the Eq. (6) include both physical viscous terms and the artificial dissipation terms. The definition of these terms as well as of coefficients  $\alpha_i$  can be found in Mavriplis, Jameson and Martinelli (1989).

### 4. ARTIFICIAL DISSIPATION

The set of equations represented by Eqs. (5) requires the addition of artificial dissipation. This is necessary because the physical viscous terms of the Navier-Stokes equations do not provide adequate levels of dissipation required by the numerical method, especially at high-Reynolds-number flows (Mavriplis, Jameson and Martinelli, 1989). For this type of flow only highly refined mesh throughout the domain provide enough damping to stabilize the numerical scheme. The usual form to stabilize this type of numerical scheme is to add an operator that is constructed by a blend of biharmonic and undivided Laplacian terms. In earlier work, the authors used a simple artificial dissipation operator. The simple operator proved adequate at the time because the computational meshes of interest were formed by triangles with low aspect ratio and the problems only considered inviscid flow simulations. However, this simple operator is not appropriate to treat viscous flow, as discussed by Mavriplis, Jameson and Martinelli (1989).

Artificial dissipation operators on unstructured mesh normally have been constructed as a blend of undivided Laplacian and biharmonic operators. The first one is responsible for efficiently capturing discontinuities and the second one to stabilize the numerical scheme in the smooth regions of the flow. A large number of tests were performed by the authors on the case of flow over a flat plate and in two-dimensional channel flows using the artificial dissipation terms presented in Dourado and Azevedo (1996). However, the modified artificial dissipation terms presented in Mavriplis, Jameson and Martinelli (1989) yielded better results for these test cases, at the expense of increased computational cost.

There are two types of regions in the domain: the convective and the viscous regions. The later occurs, for example, in the boundary layer and in high shear flow regions such as wakes. In these regions, the artificial dissipation terms must be much smaller than the physical viscous terms. For the convective dominated region, the artificial dissipation terms must also be carefully constructed to ensure the accuracy of the scheme. Other authors (Martinelli, 1987; Swanson and Turkel, 1987; Radespiel and Swanson, 1989) have demonstrated the need for different scaling of artificial dissipation terms in streamwise and normal directions in the viscous regions. The basic point is the necessity to consider the aspect ratio of the mesh near the viscous regions so

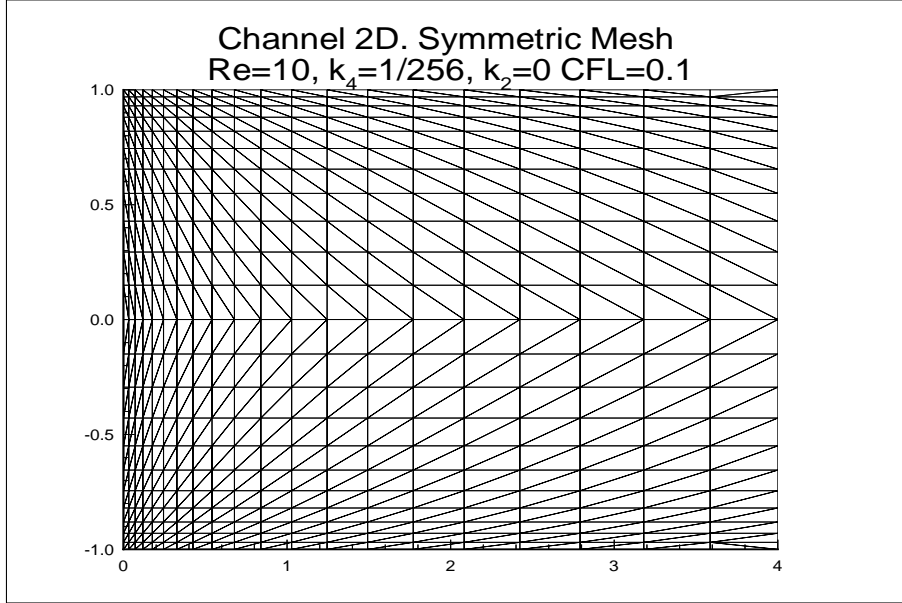


**Figure 1:** Symmetric structured triangular mesh in the 2D channel with  $L=4h$ .

that the artificial dissipation does not interfere with the physical viscous dissipation. The form proposed by Mavriplis, Jameson and Martinelli (1989) consist in adding artificial dissipation terms similar to those used in a structured mesh approach. This artificial dissipation model was implemented in this work as suggested in that report.

## 5. BOUNDARY CONDITIONS

For channel flows, constant velocity and temperature are imposed at the inlet, and the pressure is obtained by the actual solution of the equations at the boundary. In the outlet, the pressure is imposed and the other variables are obtained from the solution of the governing equations. No-slip conditions are imposed at the wall. The channel flows treated in this work would allow the definition of a symmetry plane and, hence, the solution for only half of the computational domain. However, this was not used here, and a discretization of the complete computational domain was adopted. The full domain discretization was adopted in order to avoid any influence of this type the boundary condition in the solution.

For flows over a flat plate, velocity and temperature are imposed in the far field, pressure is imposed at the outlet and no-slip conditions was imposed at the wall. Outlet type boundary condition was tried in the upper part of the domain, but the scheme became unstable. Symmetry boundary conditions were also tried and they had problems with the far field profile during the development of the boundary layer.

Special care was taken in the implementation of the artificial dissipation operator in the proximity of the boundary in order to avoid problems with the velocity profile near the wall, as reported by Dourado and Azevedo (1996). The authors solved this problem following the procedure presented by Mavriplis (1990) in which the Laplacian operator for the nodes over the wall must be calculated using projected nodes. This modification is used to ensure that there are no gradients in the normal direction provided by the artificial dissipation terms. The present investigation showed that this type of solution needs to be adopted even for the Navier-Stokes equations.

If the special treatment of the artificial dissipation operator near the boundaries is not used, the amount of artificial dissipation generated at the wall nodes is larger than the contribution which comes from the physical viscous terms. The implementation of this special artificial

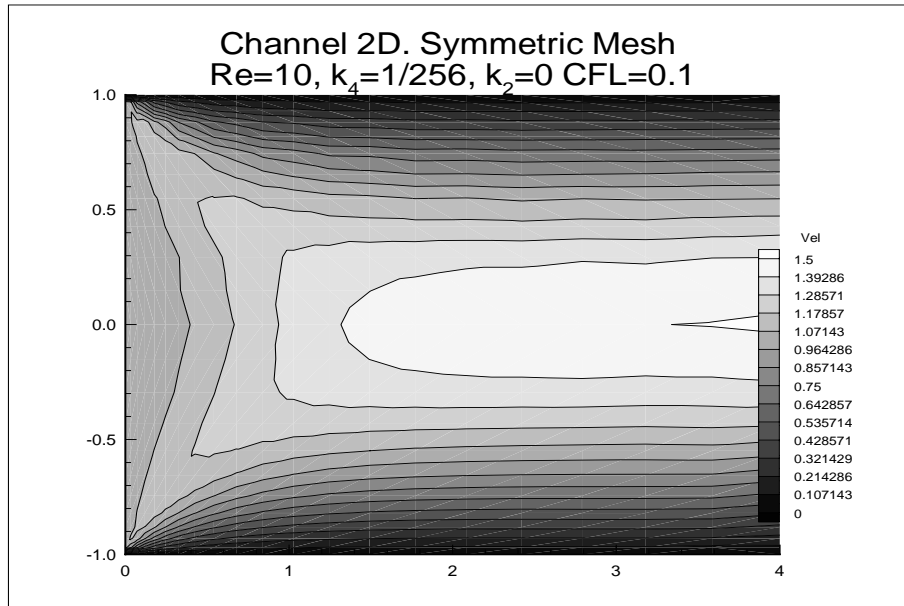


**Figure 2:** Velocity contour in the 2D channel with  $L=4h$ .

dissipation boundary scheme was adopted for all boundaries in the present work, and not only for wall boundaries as suggest by Mavriplis (1990), but the authors have not evaluated the consequences of this approach.

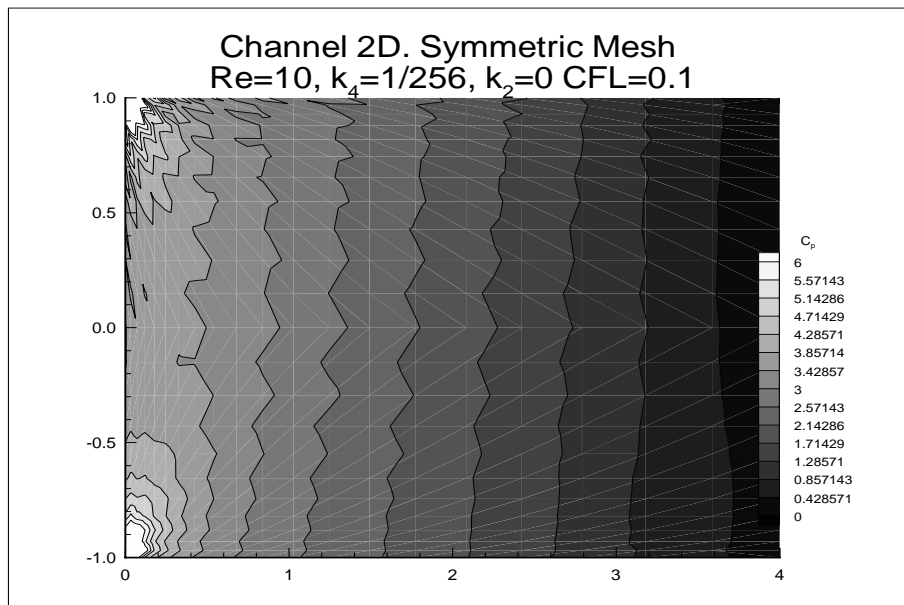


**Figure 3:** Pressure coefficient contour in the 2D channel with  $L=4h$ .

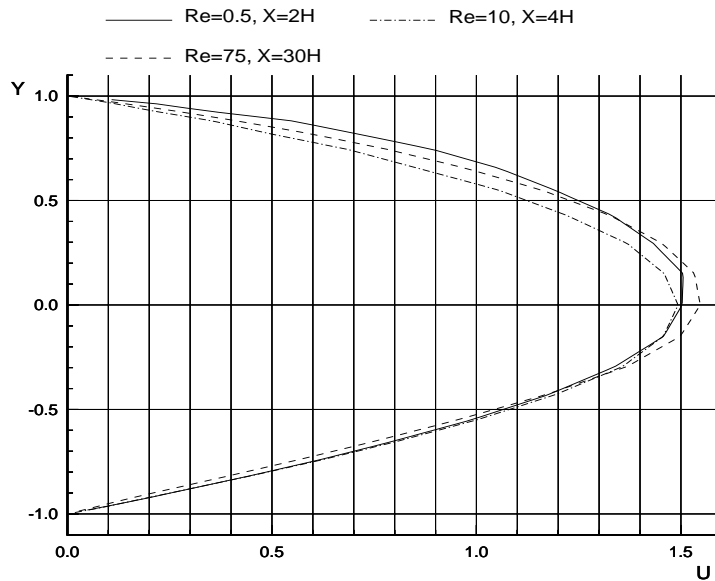
## 6. RESULTS

The scheme proposed in this work was evaluated considering two test cases, namely the external flow over a flat plate and the internal flow in a channel. The developing flowfield in a channel for three different Reynolds number was the internal flow test case selected because of the availability of data for comparison. The Reynolds numbers considered were 0.5, 10 and 75, based on the channel half height. For the external flow test case, the problem of flow over a flat

plate was evaluated and comparisons with Blasius analytical solutions were carried out.

Three different meshes were generated for the channel discretization. These meshes were obtained by triangulating over a quadrilateral structured mesh. This allows the control of the orientation of the diagonals which form the triangles from the original quadrilateral mesh. Actually, for the first triangulation, all triangles were constructed with diagonals forming a positive angle with the  $x$ -direction. It was observed, however, that the velocity profile exhibit asymmetries with regard to the channel centerline when this grid topology was adopted. Therefore, it was necessary to create symmetric meshes in order to obtain a symmetric numerical solution. One of these symmetric mesh is shown in Fig. 1. Moreover, the length of the channel varied in order to obtain fully developed velocity profile. Hence, to obtain  $Re = 0.5$ , the channel had a length of  $2h$ , where  $h$  is the channel half-height. Similarly, a channel of length  $4h$  is used in  $Re = 10$  channel test case, and a channel with length  $30h$  is used in  $Re = 75$  channel test case. The Mach number of flow in all channel test case is equal to 0.5. The particular mesh shown in Fig. 1 has total length equal to  $4h$ .

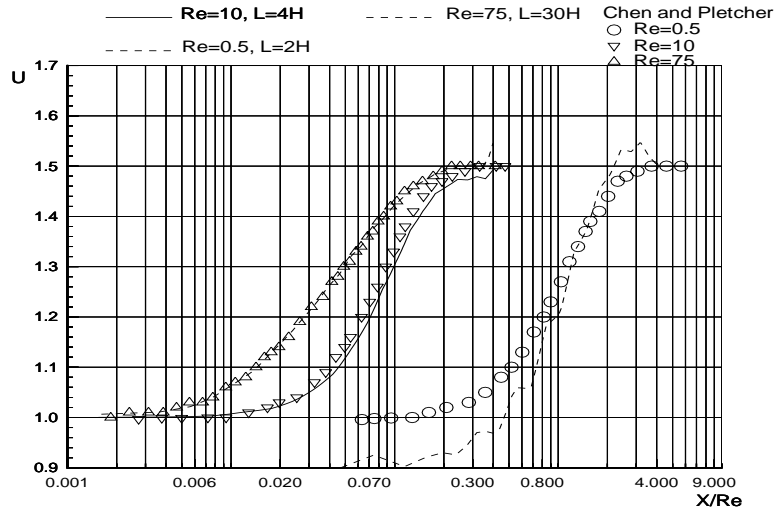
The results for the case with  $Re = 10$  are presented in Fig. 2 in terms of velocity magnitude contours. One can observe that the contour lines are fairly smooth and they are also symmetric with regard to the channel centerline. The pressure coefficient contours are shown in Fig. 3. Although these contours may seem rather ragged, one should note that they are actually a lot smoother than the corresponding results available using the artificial dissipation operator described in Dourado and Azevedo (1996). This is an indication of the improvement in resolution obtained with a more careful treatment of the artificial dissipation terms.



**Figure 4:** Velocity profile at channel end for  $Re=0.5$ , 10 and 75 and right-turned diag.

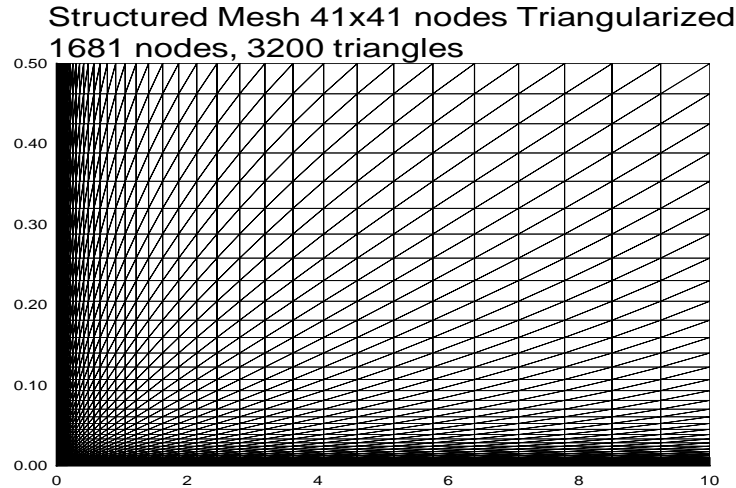
Velocity profiles at the end of the channel are shown in Fig. 4 for the three different Reynolds numbers considered in this study. The simulations for the results in Fig. 4 were run using the asymmetric grids and, hence, one can appreciate the Reynolds number effects on the solution asymmetry for this case. Apparently, the combination of the existence of a preferred direction in these grids together with the high aspect ratio triangles obtained with such meshes leads to the inaccuracies in the final converged solution. On the other hand, symmetric meshes as the one shown in Fig. 1 yield correct results for the velocity profiles.

Figure 5 presents a comparison between the present computational results and those available in Chen and Pletcher (1991). The agreement is very good for the two higher Reynolds number cases. For  $Re = 0.5$ , the agreement is not as good, but the correct trends are captured by the present calculation. It is believed at this point that further grid refinement is necessary



**Figure 5:** Center line velocity distribution for  $Re=0.5, 10$  and  $75$  against Chen and Pletcher.

in order to improve the results for  $Re = 0.5$ .



**Figure 6:** Triangular structured mesh (41x41).

The calculations for the flow over the flat plate were performed using two different mesh topologies. One of these was, again, a triangular grid obtained by triangularization over a structured mesh, whereas the other was a truly unstructured grid generated by the advancing front technique. The domain non-dimensionalization is performed using a somewhat arbitrary reference length. Using this reference length, one can define a reference Reynolds number for the test case. Hence, for each  $x$ -position along the plate, one can calculate a value of  $Re_x$  based on the dimensionless distance from the plate leading edge and on the reference Reynolds number. With this approach, the meshes used have a fixed height, as shown in Figs. 6 and 8, and the parameter which has actual physical meaning in order to determine the solution at a given longitudinal station is  $Re_x$ .

The structured meshes used for triangulation have two dimensionless heights, 0.1 and 0.5, where in Fig. 6 is possible to see an example of this type of mesh, with dimensionless height equal to 0.5. The quadrilateral structured mesh used for triangulation to produce this mesh has  $41 \times 41$  nodes. The existence of problems with the boundary layer profile was the reason which led the authors to increase the domain height of 0.1 to 0.5. Meshes with refinement both in  $x$ -direction and/or  $y$ -directions were used with this grid type and the best results which could

be obtained with this grid topology are shown in Fig. 7. These results show improvement of velocity profiles near the wall in comparison with results presented by Dourado and Azevedo (1996). This is the consequence of a better treatment of the artificial dissipation terms on the boundary.

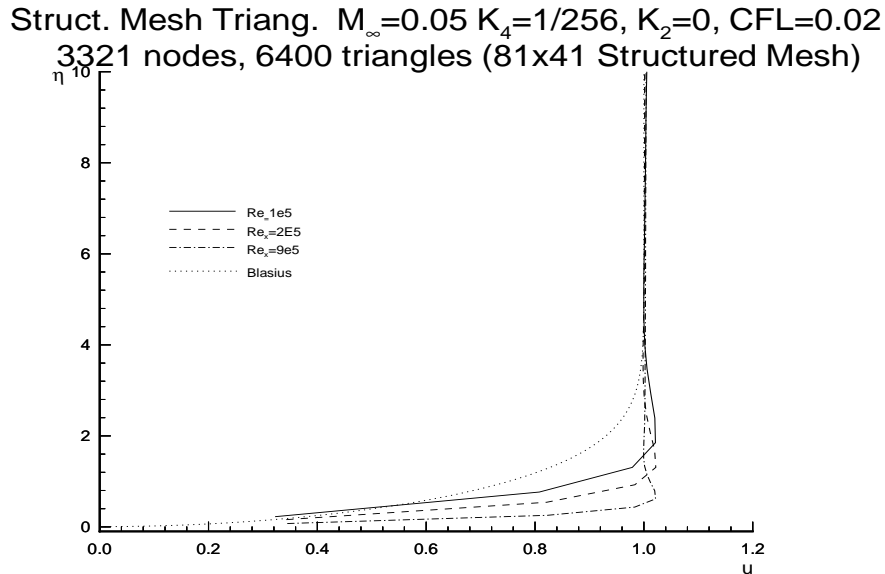


Figure 7: Presents results with 81x41 mesh and Blasius solution.

The tests with a large number of triangularized structured mesh configurations led the authors to believe that the aspect ratio influences the quality of the solution for the boundary layer profile. Then, calculations with a truly unstructured grid were also performed. This grid has localized refinement which yields a mesh with near equilateral triangles. Two grids were used, a coarse grid with 2950 nodes and 5504 triangles, and a fine grid with 27757 nodes and 52758 triangles. The fine grid was obtained by essentially refining the boundary layer region. The coarse grid is shown in Fig. 8.

A comparison of the results obtained at different plate stations, namely for  $Re_x = 500$ ,  $Re_x = 1000$  and  $Re_x = 3000$  are shown in Fig. 9 together with Blasius solution. One can see in Fig. 9 that the results for this case show a marked improvement with respect to the corresponding results obtained with the other grid topology. Apparently, the use of nearly equilateral triangles has a very positive effect on the quality of the solutions obtained. Moreover, although a curve is not shown here for brevity reasons, the friction coefficient distribution has also presented quite a good comparison with the theoretical values.

## 7. CONCLUSIONS

The results presented here show that the present numerical scheme is able to treat both internal and external viscous flows. The necessity of well constructed viscous terms is a fundamental point to treat external flows. The way of deriving the viscous terms is the basic point for construction of accurate viscous terms. The heavy computational cost penalties incurred by the need of having nearly equilateral triangles in the boundary layer indicate that, to explore all the capabilities of unstructured mesh schemes for viscous dominated flow regions, one way have to resort to hybrid mesh approach as suggested by Mavriplis (1988),(1989).

## REFERENCES

Azevedo, J. L. F., and Dourado, W. M. C., 1991, Euler solutions of two dimensional flows



## Unstructured Mesh

2950 nodes, 5504 volumes

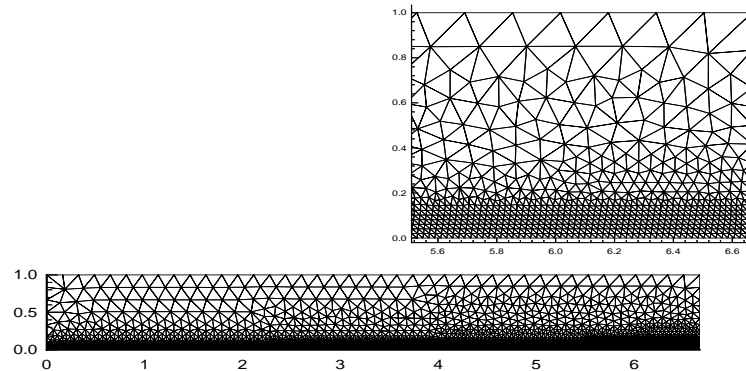


**Figure 8:** Fully unstructured mesh (coarse mesh) with 2950 nodes and 5504 triangles.

using unstructured meshes, Proceedings of the 11th Mechanical Engineering Congress - XI COBEM, December, São Paulo, SP, Brazil, Vol. “Azul”, pp. 189-192.

Azevedo, J. L. F. and Martins, R. J., 1993, Compressible and incompressible flow simulations using a finite difference method, Proceedings of the 5th International Symposium on Computational Fluid Dynamics, Aug.-Sept., Sendai, Japan, Vol. I, pp. 38-43.

Chen, K.-H. and Pletcher, R. H., 1991, Primitive variable, strongly implicit calculation procedure for viscous flows at all speed, AIAA Journal, Vol. 29, No. 8, pp. 1241-1249.

Dourado, W. M. C. and Azevedo, J. L. F., 1992, Inviscid flow solution over airfoils using finite volumes in unstructured grids, Proceedings of the 4th Brazilian Congress of Engineering (ENCIT-92), December, Rio de Janeiro, RJ, pp. 21-24 ( in Portuguese, original title is “Solução de escoamentos não-viscosos em aerofólios utilizando volumes finitos em malhas não-estruturadas”).

Dourado, W. M. C. and Azevedo, J. L. F., 1993, Simulation of high speed inviscid flows with a finite volume unstructured grid solver, Proceedings of the 12th Mechanical Engineering Congress - COBEM 93, December, Brasília, DF, Brazil, Vol. I, pp. 129-132.

Dourado, W. M. C. and Azevedo, J. L. F., 1996, Flow simulation with unstructured meshes over basic automotive configurations with all speed method, Proceedings of the 6th Brazilian Congress of Engineering and Thermal Sciences and 6th Latin American of Mass and Heat Transfer, ENCIT/LATCYM 96, November, Florianópolis, SC, Vol. I, pp. 553-558 (in Portuguese, original title is “Simulação de escoamentos com malhas não-estruturadas sobre configurações automotivas básicas com um método para toda a faixa de velocidade”).

Dourado, W. M. C., 1997, Unstructured meshes utilization for aerodynamic flows simulation, Master Thesis, Instituto Tecnológico de Aeronáutica, São José dos Campos, SP, Brazil (in Portuguese, original title is “Utilização de malhas não-estruturadas para simulação de escoamento aerodinâmico”).

Ferrari, M. A. S., 1996, Convergence acceleration for an implicit method for flows in all speed regimes, Master Thesis, Instituto Tecnológico de Aeronáutica, São José dos Campos, SP, Brazil (in Portuguese, original title is “Aceleração de convergência de um método numérico implícito para escoamentos em qualquer regime de velocidade”).

Ferrari, M. A. S., and Azevedo, J. L. F., 1995, Convergence acceleration for an implicit method for flows in all speed regimes, Proceedings of the 13th Brazilian Congress and 2nd Iberian American Congress of Mechanical Engineering - COBEM/CIDIM/95, Belo Horizonte, MG, Brazil (in Portuguese, original title is “Aceleração de convergência de um método implícito para escoamentos em qualquer regime de velocidade”).

Unstructured Mesh  $M_\infty=0.05$   $K_4=1/256$ ,  $K_2=0$ ,  $CFL=0.3$   
 27757 nodes, 52758 triangles

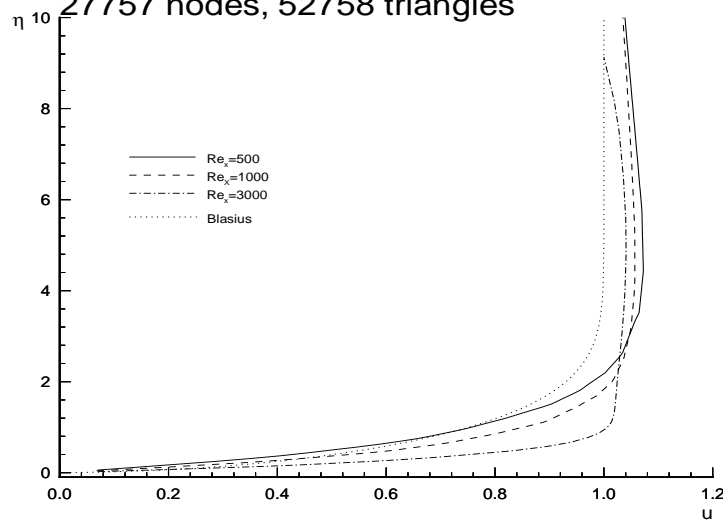


**Figure 9:** Results of fully unstructured mesh (fine mesh) with 27757 nodes and 52758 triangles.

- Giles, M. B., 1990, Nonreflecting boundary conditions for Euler equations calculation, *AIAA Journal*, Vol. 28, No. 12, pp. 2050-2058.
- Jameson, A., Schmidt, W., and Turkel, E., 1981, Numerical solutions of the Euler equations by finite-volume methods using Runge-Kutta time stepping schemes, *AIAA Paper* 81-1259.
- Jameson, A., and Mavriplis, D., 1986, Finite volume solution of the two-dimensional Euler equations on a regular triangular mesh, *AIAA Journal*, Vol. 24, pp. 611-618.
- Martinelli, L., 1987, Calculations of viscous flows with a multigrid method, Ph.D. Thesis, Princeton University, Princeton, USA.
- Martins, R. J., and Azevedo, J. L. F., 1993, A finite difference method for flow simulation at all speeds, *Proceedings of the 12th Brazilian Mechanical Engineering Congress - COBEM 93*, December, Brasília, DF, Brazil, Vol. I, pp. 105-108.
- Martins, R. J., 1994, A finite difference method for flow simulation at all speeds, Master Thesis, Instituto Tecnológico de Aeronáutica, São José dos Campos, SP, Brazil ( in Portuguese, original title is "Um método de diferenças finitas para simulação de escoamentos em qualquer regime de velocidade").
- Mavriplis, D., 1988, Multigrid solution of the two-dimensional Euler equations on unstructured triangular meshes, *AIAA Journal*, Vol. 26, No. 7, pp. 824-831.
- Mavriplis, D., 1990, Accurate multigrid solution of the Euler equations on unstructured and adaptive meshes, *AIAA Journal*, Vol. 28, No. 2, pp. 213-221.
- Mavriplis, D., 1995, A unified multigrid solver for the Navier-Stokes equations on mixed element meshes, *AIAA Paper* 95-1666.
- Mavriplis, D., 1998, Multigrid strategies for viscous flow solvers on anisotropic unstructured meshes, *Institute for Computer Applications in Science and Engineering Rept.* 98-6.
- Mavriplis, D., Jameson, and A. Martinelli, L., 1989, Multigrid solution of the Navier-Stokes equations on triangular meshes, *Institute for Computer Applications in Science and Engineering Rept.* 89-11.
- Swanson, R. C., and Turkel, E., 1987, Artificial dissipation and central difference schemes for the Euler and Navier-Stokes Equations, *AIAA paper* 87-1107, *AIAA 8th Computational Fluid Dynamics Conference*, June, Honolulu, Hawaii.
- Radespiel, R., and Swanson, R. C., 1989, An investigation of cell centered and cell vertex multigrid schemes for the Navier-Stokes equations, *AIAA paper* 89-0543, *AIAA 27th Aerospace Sciences Meeting*, January, Reno, Nevada.